

Combining Remotely Sensed Data and Ground-Based Radiometers to Estimate Crop Cover and Surface Temperatures at Daily Time Steps

A. N. French¹; D. J. Hunsaker²; T. R. Clarke³; G. J. Fitzgerald⁴; and P. J. Pinter Jr.⁵

Abstract: Estimation of evapotranspiration (ET) is important for monitoring crop water stress and for developing decision support systems for irrigation scheduling. Techniques to estimate ET have been available for many years, while more recently remote sensing data have extended ET into a spatially distributed context. However, remote sensing data cannot be easily used in decision systems if they are not available frequently. For many crops ET estimates are needed at intervals of a week or less, but unfortunately due to cost, weather, and sensor availability constraints, high resolution (<100 m) remote sensing data are usually available no more frequently than 2 weeks. Since resolution of this problem is unlikely to occur soon, a modeling approach has been developed to extrapolate remotely sensed inputs needed to estimate ET. The approach accomplishes this by combining time-series observations from ground-based radiometers and meteorological instruments with episodic visible, near infrared, and thermal infrared remote sensing image data. The key components of the model are a vegetation density predictor and a diurnal land surface temperature disaggregator, both of which supply needed inputs to a surface energy balance model. To illustrate model implementation, remote sensing and ground-based experimental data were collected for cotton grown in 2003 at Maricopa, Ariz. Spatially distributed cotton canopy densities were forecasted for a 22-day interval using vegetation indices from remote sensing and fractional cover from ground-level photography. Spatially distributed canopy and soil surface temperatures were predicted at 15-min time steps for the same interval by scaling diurnal canopy temperatures according to time of day and vegetative cover. Considering that the predictions span a rapid growth phase of the cotton crop, comparison of spatially projected canopy cover with observed cover were reasonably good, with $R^2=0.65$ and a root-mean-squared error (RMSE) of 0.13. Comparison of predicted temperatures also showed fair agreement with RMSE=2.1 °C. These results show that combining episodic remotely sensed data with continuous ground-based radiometric data are a technically feasible way to forecast spatially distributed input data needed for ET modeling over crops.

DOI: 10.1061/(ASCE)IR.1943-4774.0000169

CE Database subject headings: Evapotranspiration; Remote sensing; Temperature effects; Arizona.

Author keywords: Evapotranspiration.

Introduction

Accurate estimation of evapotranspiration (ET) is important for many applications where water supplies are scarce. For irrigated agriculture in particular, knowledge of ET is especially important for effective water scheduling and management (Howell 1996; Jensen et al. 1990). Several well-established ET estimation approaches that exist are consistent and can perform well for homo-

geneous crop cover and optimum agronomic management. Among these, the most commonly used for irrigation scheduling purposes is the crop coefficient (K_c)/reference ET method (Jensen and Allen 2000), such as those in Food and Agriculture Organization of the United Nations [Food and Agriculture Organization (FAO)]-24 (Doorenbos and Pruitt 1977) and FAO-56 (Allen et al. 1998). However, ET predictions for K_c -based approaches are subject to considerable inaccuracies where vegetation is spatially variable or where—despite its apparent uniformity—vegetation is stressed from salinity or water deficit (Martin and Gilley 1993; Allen et al. 2005; Hunsaker et al. 2005).

The only practical way to consider effects of spatial variability upon ET is to use remotely sensed images, which can potentially observe changes in land cover at submeter scales. Many contributions, particularly those employing thermal infrared observations, have shown how remote sensing techniques could be used operationally (Bartholic et al. 1970; Brown and Rosenberg 1973; Jackson et al. 1977; Soer 1980; Seguin and Itier 1983; Hatfield et al. 1984; Mecikalski et al. 1999). Although sensors such as Landsat and ASTER provide the necessary resolution (15–90 m) to distinguish between land cover types, the temporal repetition rate is rarely better than 16 days. For crop applications at farm scales, where critical irrigation decision intervals are short, it is likely that such infrequent image data would have limited value.

¹Research Physical Scientist, U.S. Arid Land Agricultural Research Center, USDA/ARS, 21881 North Cardon Lane, Maricopa, AZ 85138 (corresponding author). E-mail: andrew.french@ars.usda.gov

²Agricultural Engineer, U.S. Arid Land Agricultural Research Center, USDA/ARS, Maricopa, AZ 85138.

³Physical Scientist, U.S. Arid Land Agricultural Research Center, USDA/ARS, Maricopa, AZ 85138.

⁴Senior Scientist, Dept. of Primary Industries, Horsham, Victoria 3401, Australia.

⁵Research Collaborator, U.S. Arid Land Agricultural Research Center, USDA/ARS, Maricopa, AZ 85138.

Note. This manuscript was submitted on November 1, 2008; approved on August 20, 2009; published online on September 3, 2009. Discussion period open until September 1, 2010; separate discussions must be submitted for individual papers. This paper is part of the *Journal of Irrigation and Drainage Engineering*, Vol. 136, No. 4, April 1, 2010. ©ASCE, ISSN 0733-9437/2010/4-232–239/\$25.00.

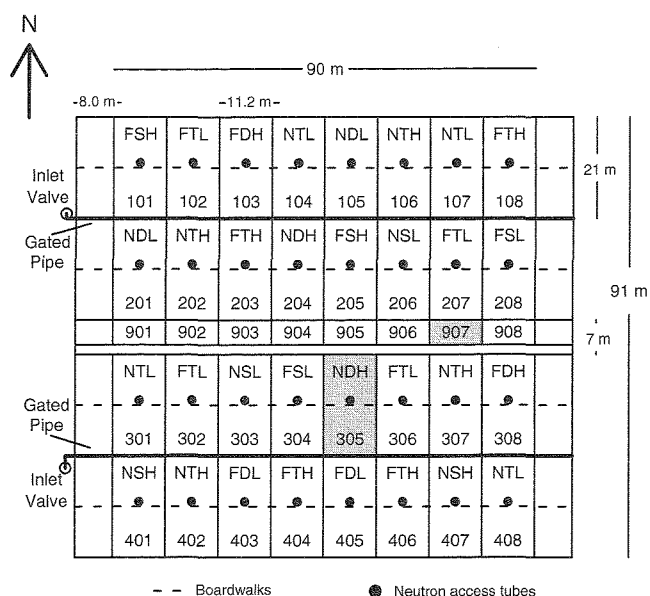


Fig. 1. FISE03 experimental layout for cotton grown at Maricopa, Ariz. in 2003

Clearly, more frequent repeat periods for higher resolution satellite sensors are needed. Such platforms do exist, examples of which are Rapid Eye (www.rapideye.de); QuickBird (www.digitalglobe.com); and SPOT (www.spot.com), but in these instances thermal infrared data are not available (Anderson and Kustas 2008). Furthermore, agricultural users are constrained by image acquisition costs, cloudy skies, and limited spatial coverage. Future platforms are being proposed that would have repeat intervals as short as 1 week, for example, a high-resolution instrument with a multispectral thermal infrared capability (hyspirc.jpl.nasa.gov).

Recognizing that for the foreseeable future, remote sensing data of the type, quality, cost, and frequency needed for crop water management will likely not be available, a remote sensing estimation approach is proposed that uses a combination of remote sensing images and ground-based, fixed-location radiometers. In the approach, spatially distributed information is provided from image data, while time-series information is provided from ground-based radiometers. In this proposed scheme, time-series maps of vegetation cover and surface temperatures can be generated for frequent time intervals (e.g., 1/4 hour) and ultimately can be used as inputs to a surface energy balance model.

FISE03 Experiment

To demonstrate the proposed model (elaborated in the next section), experimental data were used from an intensive cotton field experiment known as FAO Irrigation Scheduling Experiment 2003 (FISE03, Hunsaker et al. 2005). FISE03 included a ground field site with associated meteorological, soil, agronomic, and hydrologic instruments, plus 10 remote sensing overflights using a helicopter-based platform.

The site (Fig. 1) is a 1.3 ha field at the University of Arizona Maricopa Agricultural Center (MAC) approximately 50 km south of Phoenix, Ariz. (33.067°N, 111.967°W, 361 m above sea level). For the 2003 experiment, cotton was planted in a 4 by 8 matrix of 32 randomized 11.2 m × 21 m plots. Plots were identified by three digit numbers, ranging between 101 and 408, and

also by three-letter codes. The numbering scheme denotes row and column positions for each plot, while the letter codes denote experimental treatments. These codes identify the irrigation scheduling scheme ["F" and "N": FAO versus normalized difference vegetation index (NDVI) approaches]; the planting density ("S," "T," and "D": sparse, typical, and dense); and nitrogen levels ("L" and "H": low and high). Additional plots, numbered 901–908 and located within the middle of the site, were not a main part of the experimental design but did provide important surface temperature data for unvegetated dry and wet soil conditions. See Hunsaker et al. (2005) for details.

Deltapine 458BR (*Gossypium hirsutum* L.), a mid-to-full maturing transgenic cotton variety grown in the state, was planted at the field site on April 7 and 8, 2003. A four-row planter (Model 1700, Deere and Co., Moline, Ill.), calibrated at a rate of 10 cotton seeds m⁻², was used to plant single rows of seed in the center of the bed (1.016-m bed spacing) for both the T and S density plots (the sparse treatment plots were later hand thinned to 5 plants/m² after emergence). Dense plots (20 plants/m²) were planted with a Monosem twin-row precision vacuum planter (Model NG, A.T.I., Inc., Lenexa, Kan.) at 0.2-m spacing along the bed. As described in Hunsaker et al. (2005), after the cotton was established, irrigation scheduling was predicated on replacing 1.1 times estimated ET when soil water depletion from the root zone reached a level of 45%. The estimated daily ET was calculated for all plots using the FAO-56 dual crop coefficient procedures (Allen et al. 1998). All FAO plots were irrigated according to a single basal crop coefficient (K_{cb}) curve, whereas the crop coefficients for NDVI plots were generated separately for each plot using ground-based NDVI measurements and a previously developed relationship between K_{cb} and NDVI. Nitrogen applications for the high N level plots followed locally recommended practices for cotton (Doerge et al. 1991), predicated on leaf petiole nitrate content levels that were periodically monitored in the plots during the season. All high N plots received a total seasonal application of 112 kg N ha⁻¹, whereas no N was applied to the L plots. Final yields were obtained from seed cotton that was hand-picked within a final harvest area measuring approximately 24 m² in the south half of each plot and then ginned at MAC.

A primary objective of FISE03 was development of remote sensing-based irrigation scheduling techniques, and consequently the collected data were valuable for remote sensing forecasting too. Specifically, the water budget was monitored in detail, allowing ET estimation on a plot by plot basis at daily to weekly time scales. The plots were flood irrigated with each surrounded by border dikes, where soil volumetric moisture contents were systematically measured immediately prior to, following, and between irrigation events from 3 m deep access tubes near the centers of each of the 32 plots. At each location, neutron scattering data from a field-calibrated Campbell Pacific Nuclear instrument were combined with a time domain reflectometer (Soil-Moisture Equip. Corp.) to return soil water content between the surface and 2.8-m depths. This range of depths allowed monitoring of shallow soil evaporation, root-zone uptake, and soil water loss from infiltration at the plot center.

Meteorological and land surface temperature data collected at FISE03 included one Eppley 8–48, solar radiometer, two R.M. Young photochopper type anemometers at a height of 2 m, air temperature (dry and wet bulb), aspirated USDA/ARS-designed ceramic wick psychrometers, and a Texas Electronics rain gauge.

To monitor soil and plant canopy temperatures, infrared thermometers were deployed in 11 plot locations at different times during the cotton growing season. The thermometers were Ever-

est (Everest Interscience, Tucson, Ariz.) Models 3073 and 3500, and Apogee (Apogee Instruments, Logan, Utah) IRT model IRT-P5. Of these, nine were pointed toward cotton plants at $\sim 30^\circ$ from horizontal, and two were pointed toward bare soil at $\sim 60^\circ$ from horizontal. These angles were chosen to maximize the canopy and soil signals while reducing effects from instrument mounts.

Remote sensing data at FISE03 were collected on 10 occasions between May 7, 2003 and October 13, 2003 using a helicopter platform. This study used remote sensing data acquired on June 17 and July 9 [i.e., Day of Year (DOY) 168 and 190]. Data acquired were of two kinds: surface temperatures from a thermal infrared camera and vegetation indices from a visible-near infrared camera.

The temperature images were acquired by a FLIR Systems SC2000 thermal camera (FLIR Systems AB, Danderyd, Sweden), which contained a dynamically calibrated microbolometer detector 240×320 array with 1.3×10^{-3} rad pixel instantaneous field of view. Considering the 760-m flight elevation, effective resolution was ~ 1 m. For compatibility with higher resolution visible near infrared (VNIR) data, the FLIR data were subsampled to 0.5 m. The specific camera used was band pass filtered between 10.0 and $13.0 \mu\text{m}$ to reduce errors from highly variable emissivities commonly encountered at shorter wavelengths. Calibration tests showed accuracies $< 1.0^\circ\text{C}$ for controlled conditions.

The vegetation index image data were acquired from a Duncan MS3100, 8-bit, three-band camera (Redlake, Tucson, Ariz.), with detectors for a red band at 670 nm, a far-red band at 720 nm, and a near infrared band at 790 nm, each at full-wave-half-maximum of 10 nm. NDVI was constructed from the red and near infrared reflectances. Prior to this construction, reflectance data were created from Duncan imagery by normalization against four 8×8 m field deployed calibration tarps (Group VIII Technologies, Provo, Utah) using procedures similar to that described in Moran et al. (2001). These tarps had nominal reflectance values of 4, 8, 48, and 64%.

Last, to improve estimation of fractional cover, weekly nadir-viewing photographs of cotton were collected throughout the field. These were obtained with a conventional film camera mounted on a hand-carried pole ~ 2 m long and diagonally positioned 1 m south of midfield access boardwalks (Fig. 1). Green:red ratio images were created from the digitized images and used to generate sample estimates of fractional cover (French et al. 2009).

Forecasting Remotely Sensed Cover and Land Surface Temperature

The remote sensing forecasting method consists of three main components:

1. A temperature-based remote sensing surface energy balance model that computes net radiation, sensible heat flux, soil heat flux, and latent heat flux;
2. A vegetation density submodel that can forecast changing crop cover at daily time steps using remotely sensed vegetation indices; and
3. A land surface temperature submodel that can forecast canopy and soil temperatures at minute to hourly time steps using ground-based radiometers.

This study considers the latter two components, energy balance model input data. When these inputs are combined, it becomes feasible to estimate spatially distributed ET at frequent

time steps for a few weeks following acquisition of remote sensing image data.

Energy Balance Model

To understand the rationale for modeling extrapolated cover and land surface temperatures, a brief description of a temperature-based surface energy balance model is needed. Remote sensing surface energy balance models estimate ET by modeling the four most important energy flux components: net radiation: R_n , soil heat: G , sensible heat: H , and latent heat: LE

$$R_n - G = H + LE \quad (1)$$

where the left hand side represents available energy flux and the right hand side represents turbulent flux. Instantaneous ET (in terms of liquid water depth) is obtained by solving Eq. (1) for LE and dividing by the product of water density and the latent heat of vaporization. Estimation of ET at daily time steps requires additional assumptions or information. One common approach assumes constant evaporative fraction for the day (Lhomme and Elguero 1999). However for the proposed spatial estimation method, LE estimates could be available at frequent time steps (i.e., 15 min in this study) so that daily ET is estimated from a summation over a 24-h period.

Given frequent input values, a variety of energy balance modeling approaches could be used. Examples of documented methods include SEBAL/Metric (Bastiaanssen et al. 1998; Allen et al. 2007), the surface energy balance system, Su (2002), a water deficit estimator (Moran et al. 1994), and the vegetation-temperature triangle approach (Carlson et al. 1994, 1995). For this study a form of the two source energy balance (TSEB) model (Norman et al. 1995) was chosen because the proposed temperature disaggregation approach is well suited to the two source methodology. A distinguishing feature of TSEB is its computation of LE in two energy flux streams: one for the vegetation canopy and another for the soil surface.

Doing so allows for better modeling of available radiative energy and parameterization of aerodynamic transport resistances. Using the spatial estimation approach to be described, TSEB can be implemented as described in Norman et al. (1995), except that canopy temperatures do not need the Priestley-Taylor constraint (Priestley and Taylor 1972) since they are directly estimated from observations.

Vegetation Density Model

One of the chief values of remote sensing image data are the ability to generate maps of spatial vegetation cover density throughout the fields of interest. Knowledge of cover density is important for energy balance models such as TSEB since it is used to estimate partitioning of net radiation and constrain canopy transpiration. Remote sensing of canopy cover can be accomplished with the construction of a vegetation index, such as the NDVI (Rouse et al., 1973). Correspondence between cover and NDVI, though imprecise, is established empirically, for example, with the squared scaled NDVI relationship described by Carlson et al. (1995), or semiempirically through a power function relation described by Choudhury (1987) and Choudhury et al. (1994).

In the current study, the Choudhury approach was implemented using remote sensing image data

Cotton Fractional Cover Estimation

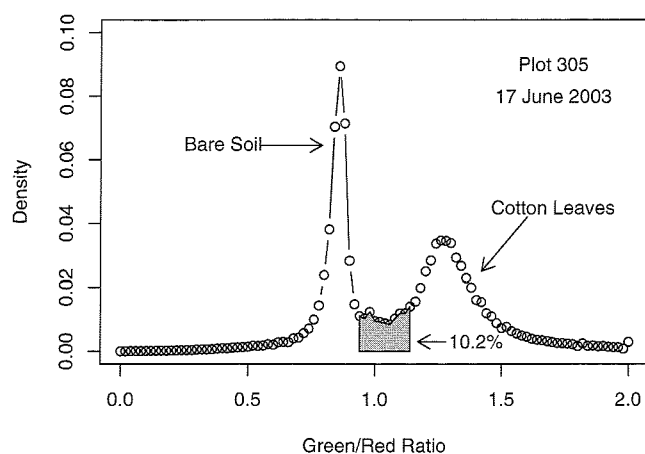


Fig. 2. Histogram of the green/red ratio for a nadir-viewing photograph taken of cotton growing in experimental plot 305 on June 17, 2003 (DOY 168). The bimodal distribution allows accurate discrimination between bare soil (which has a dominant red color) and cotton leaves. The confusion interval (ratio 0.98–1.1) was found to include 10.2% of the image pixels.

$$f = 1 - \left[\frac{\text{NDVI}_{mx} - \text{NDVI}}{\text{NDVI}_{mx} - \text{NDVI}_{mn}} \right]^p \quad (2)$$

where f represents fractional vegetation cover; NDVI_{mx} represents full cover; NDVI_{mn} represents bare soil; and the exponent p is a function of leaf orientation distributions within a canopy. p ranges between 1.25 for planophile canopies to <0.7 for erectophile canopies; for the current study 1.0 was used. Thus Eq. (2) allows transformation of remotely sensed NDVI data into spatially distributed estimates of fractional cover.

To provide the best possible estimates of cover, Eq. (2) was calibrated using nadir-view photography previously mentioned in the FISE03 Experiment section. In an operational setting such an approach would probably be impractical, and in such cases forecast mean cover would have to rely upon generalized calibrations of Eq. (2). But at FISE03, use of the technique was a research tool designed to seek the best possible fractional cover estimates. Implementation of the method was straightforward and empirical: using green and red bands from high-quality photographs, histograms of the green:red ratio created from image samples collected throughout the field were constructed and a threshold value was chosen to best divide the bimodal distributional pattern (Fig. 2). Soil conditions in other settings might not allow good separation but at Maricopa the reddish soil contrasted strongly against green leaves. The chosen threshold evenly divided the bimodal pattern representing soil and vegetation. Fractional cover was then obtained by summing all image pixel values greater than the threshold and dividing by the total number of sampled pixels. In this instance cover classification uncertainty, corresponding to values between the peaks was $\sim 5\%$.

To construct maps of predicted spatially distributed cover, the approach assumed that the range of cover values could be dynamically modeled with a smooth statistical distribution function for locally specified management zones. For each zone, predicted spatial patterns were modeled by using estimates of mean cover and observations of spatially distributed NDVI from the recently available remote sensing image data.

FISE03 Cotton (All Plots)

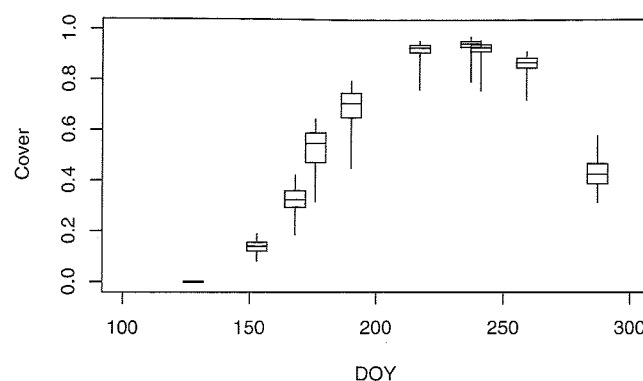


Fig. 3. Fractional cover for cotton in all FISE03 plots. The box symbols display the median and interquartile range of cover, while the whiskers display the 95th percentile range. Note that cover variability increases twice during a growing season: once during the growth phase (\sim DOY 176 or June 25), and again during senescence ($>$ DOY 250 or September 7).

The chosen function for this study was the Beta distribution which is a bounded but flexible distribution function that can be adapted to a wide range of patterns using only two shape parameters (α and β). For unimodal distribution patterns both parameters will be >1 , with $\alpha < \beta$ for sparse cover, and $\alpha > \beta$ for dense cover. Because the bounds for cover are the same for the standard Beta function (i.e., 0 to 1), no change of scales was necessary.

The Beta shape parameters α and β were computed using the method-of-moment estimators

$$\alpha = \bar{f} \left[\frac{\bar{f}(1 - \bar{f})}{f_{\text{var}}} - 1 \right] \quad (3)$$

$$\beta = (1 - \bar{f}) \left[\frac{\bar{f}(1 - \bar{f})}{f_{\text{var}}} - 1 \right] \quad (4)$$

For existing remote sensing image data, estimation of α and β factors follows directly from observed cover means and variances. For times beyond the most recent remote sensing data, assumed values for \bar{f} and f_{var} were needed.

For this study, mean cover estimates were obtained from previously mentioned nadir-view photographs, while cover variance was assumed to be the same as observed within the most recently available remote sensing image. As shown in Fig. 3, assuming constant cover variance was reasonable for short time intervals, but less so when considering the full growing season. At FISE03, variance of cotton cover increased two times: once during the midgrowth phase and again during senescence. However, these variance changes were slow at fortnightly prediction time scales and thus consequent errors from the constancy assumption were small.

Once Beta shape factors were known for both the remote sensing image data acquisition time and for the forecast time, predicted cover was computed by assuming that the quantile for each pixel cover value did not change. Hence, even though mean cover values did change with time, the cover distribution could be predicted by using the remote sensing-based cover quantiles with the forecast shape parameters α and β .

To illustrate the procedure, mean fractional cover estimates, obtained from nadir-view photography over one experimental plot

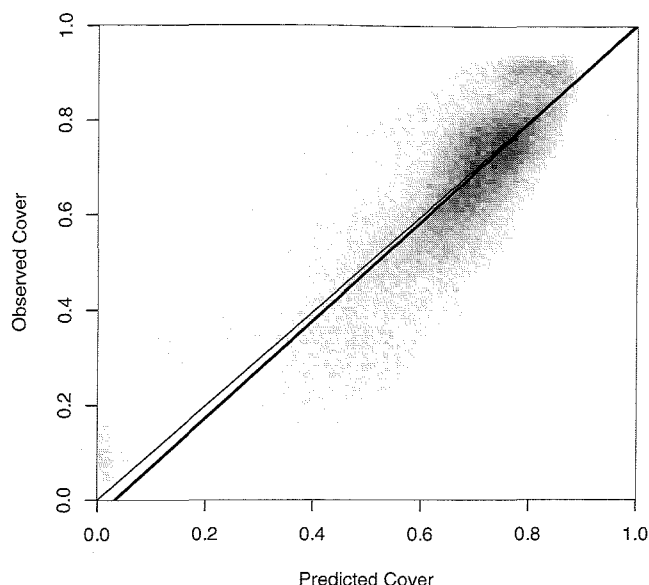


Fig. 9. Observed versus predicted cotton canopy cover on DOY 190 (July 2003). Shading indicates count frequencies where dark tones represent the highest counts. The 1:1 line indicates 10% prediction accuracy for cover exceeding 65%. Results for sparser cover were biased by 20%.

Discussion

Outcomes from initial experimentation with an airborne and ground-based image forecasting system show that land surface temperatures and vegetative cover can be forecasted reasonably accurate for 2-week time intervals during a rapid growth phase of a cotton crop. This time interval corresponds closely to typical repeat periods for sun-synchronous satellites, which are likely the only remote sensing platform for routine agricultural applications. The prime motivation for this approach was to provide the needed inputs for modeling ET when remote sensing image data are unavailable. A result of this study was a demonstration of its technical feasibility. Whether or not the approach is operationally feasible, however, requires a more comprehensive study, including economic analyses.

Clearly, no modeling procedure can replace actual remote sensing data, nor can the procedures accurately locate crop water stress unless specific ground-based observations are available for such conditions. Nonetheless, the modeling procedures do provide a mechanism to predict the best estimated daily ET when such data are otherwise unavailable. Moreover, the synthetic images represent hour-by-hour weather and radiative conditions unlikely to ever be available from a remote sensing platform. Hence daily ET estimates can be obtained from summing frequent ET estimates instead of extrapolating instantaneous ET estimates using constant evaporative fraction assumptions (e.g., Lhomme and Elguero 1999).

Model limitations were also indicated by this study, wherein predicted temperatures and vegetation cover showed discrepancies with actual observations. For the FISE03 study, land surface temperatures were not always correlative with fractional cover, a condition possibly due to crop row structure, wherein subcanopy soil temperatures were significantly different from uncovered soil temperatures. This lack of correlation could also result from using nonrepresentative remote sensing images. For example, image

data collected during an irrigation event would bias model estimates for other times. Absent additional field information, however, future implementations would require statistical constraints to ensure model robustness.

Conclusions

A remote sensing modeling approach has been developed to reduce problems estimating ET when image data are sparse. The approach forecasts crop cover density and surface temperatures after initialization by a remote sensing scene. The forecasting was accomplished by combining spatially distributed information from an airborne remote sensor with time-series radiometric observations from the ground. In this way vegetation cover could be estimated at daily time steps and surface temperatures can be estimated at subhourly time steps. The forecast approach was tested for a 22-day period using data collected over a cotton crop at an experimental site (FISE03) in Maricopa, Ariz. Spatially and temporally distributed (at 1/4 hourly intervals) surface temperatures compared acceptably with airborne observations, where the RMSE was 2.1°C and mean bias 0.4°C. Spatially distributed vegetation indices observed on June 17, 2003 were converted to fractional cover and modeled up to the next available remote sensing observation on July 9. The forecast indices agreed reasonably with actual observations where linear regression results showed $R^2=0.65$ and an RMSE of 0.65. These results indicate the subsequent modeling with synthesized image data could produce accurate daily ET estimates when high-quality remote sensing data are unavailable. Unfortunately, equivalent data from spaceborne platforms are not routinely available, and thus airborne platforms are needed for current research. Future investigations will be needed to assess the impact of the approach upon ET modeling, its validity for all parts of the growing season, and its applicability to other locations and crops.

References

- Allen, R., Clemmens, A., Burt, C., Solomon, K., and O'Halloran, T. (2005). "Prediction accuracy for projectwide evapotranspiration using crop coefficients and reference evapotranspiration." *J. Irrig. Drain. Eng.*, 131(1), 24–36.
- Allen, R. G., Pereira, L. S., Raes, D., and Smith, M. (1998). "Crop evapotranspiration: Guidelines for computing crop water requirements." *FAO irrigation and drainage paper 56*, Food and Agriculture Organization of the United Nations, Rome.
- Allen, R. G., Tasumi, M., and Trezza, R. (2007). "Satellite-based energy balance for mapping evapotranspiration with internalized calibration (METRIC)-model." *J. Irrig. Drain. Eng.*, 133(4), 380–394.
- Anderson, M., and Kustas, W. (2008). "Thermal remote sensing of drought and evapotranspiration." *EOS Trans. Am. Geophys. Union*, 89(26), 233–234.
- Bartholic, J. F., Namken, L. N., and Wiegand, C. L. (1970). "Combination equations used to calculate evaporation and potential evaporation." *Technical Rep. No. 41-170*, USDA-ARS-Bull., United States Department of Agriculture, Washington, D.C., 14.
- Bastiaanssen, W., Menenti, M., Feddes, R., and Holtslag, A. (1998). "A remote sensing surface energy balance algorithm for land (SEBAL). 1: Formulation." *J. Hydrol.*, 212–213, 198–212.
- Brown, K., and Rosenberg, N. (1973). "A resistance model to predict evapotranspiration and its application to a sugar beet field." *Agron. J.*, 65, 341–347.
- Carlson, T., Capehart, W., and Gillies, R. (1995). "A new look at the simplified method for remote sensing of daily evapotranspiration."

- Agric. For. Meteorol.*, 54, 161–167.
- Carlson, T., Gillies, R., and Perry, E. (1994). "A method to make use of thermal infrared temperature and NDVI measurements to infer soil water content and fractional vegetation cover." *Remote Sens. Rev.*, 52, 45–59.
- Choudhury, B. J. (1987). "Relationships between vegetation indices, radiation absorption, and net photosynthesis evaluated by a sensitivity analysis." *Remote Sens. Environ.*, 22, 209–233.
- Choudhury, B. J., Ahmed, N. U., Idso, S. B., Reginato, R. J., and Daughtry, C. (1994). "Relations between evaporation coefficients and vegetation indices studied by model simulations." *Remote Sens. Environ.*, 50, 1–17.
- Doerge, T., Roth, R., and Gardner, B. (1991). *Nitrogen fertilizer management in Arizona*, College of Agriculture, Univ. of Arizona, Tucson, Ariz.
- Doorenbos, J., and Pruitt, W. (1977). *Crop water requirements, irrigation and drainage 24*, Food and Agriculture Organization of the United Nations, Rome.
- French, A., Hunsaker, D., Thorp, K., and Clarke, T. (2009). "Evapotranspiration over a camelina crop at Maricopa, Arizona." *Ind. Crops Prod.*, 29(2–3), 289–300.
- Hatfield, J., Reginato, R., and Idso, S. (1984). "Evaluation of canopy temperature-evapotranspiration models over various crops." *Agric. Forest Meteorol.*, 32, 41–53.
- Howell, T. (1996). "Irrigation scheduling research and its impact on water use." *Proc., Int. Conf. on Evapotranspiration and Irrigation Scheduling*, C. Camp, E. Sadler, and R. Yoder, eds., ASAE, St. Joseph, Mich., 21–33.
- Hunsaker, D. J., Barnes, E. M., Clarke, T. R., Fitzgerald, G. J., Paul, J., and Pinter, J. (2005). "Cotton irrigation scheduling using remotely-sensed and FAO-56 basal crop coefficients." *Trans. ASAE*, 22(4), 1395–1407.
- Jackson, R., Reginato, R., and Idso, S. (1977). "Wheat canopy temperature: a practical tool for evaluating water requirements." *Water Resour. Res.*, 13, 651–656.
- Jensen, M., and Allen, R. (2000). "Evolution of practical ET estimating methods." R. Evans, B. Benham, and T. Trooien, eds., *Proc., 4th Nat. Irrig. Symp.*, American Society of Agricultural Engineers, St. Joseph, Mich., 52–65.
- Jensen, M., Burman, R., and Allen, R. (1990). "Evapotranspiration and irrigation water requirements." *ASCE manuals and reports on engineering practice 70*, ASCE, Reston, Va.
- Lhomme, J.-P., and Elguero, E. (1999). "Examination of evaporative fraction diurnal behaviour using a soil-vegetation model coupled with a mixed-layer model." *Hydrology Earth Syst. Sci.*, 3(2), 259–270.
- Martin, D., and Gilley, J. (1993). "Chapter 2, Part 623: Irrigation water requirements." *National engineering handbook*, USDA-SCS, Washington, D.C.
- Mecikalski, J., Diak, G., Anderson, M., and Norman, J. (1999). "Estimating fluxes on continental scales using remotely sensed data in an atmospheric-land exchange model." *J. Appl. Meteorol.*, 38(9), 1352–1369.
- Moran, M., Clarke, T., Inoue, Y., and Vidal, A. (1994). "Estimating crop water deficit using the relation between surface-air temperature and spectral vegetation index." *Remote Sens. Environ.*, 49, 246–263.
- Moran, M. S., Bryant, R. B., Clarke, T. R., and Qi, J. (2001). "Deployment and calibration of reference reflectance tarps for use with airborne imaging sensors." *Photogramm. Eng. Remote Sens.*, 67(3), 273–286.
- Norman, J., Kustas, W., and Humes, K. (1995). "A two-source approach for estimating soil and vegetation energy fluxes from observations of directional radiometric surface temperature." *Agric. Forest Meteorol.*, 77, 263–293.
- Priestley, C., and Taylor, R. (1972). "On the assessment of surface heat flux and evaporation using large-scale parameters." *Mon. Weather Rev.*, 100, 81–92.
- Rouse, J., Haas, R., Schell, J., and Deering, D. (1973). "Monitoring vegetation systems in the Great Plains with third ERTS." *ERTS Symp.*, Vol. SP-351, National Aeronautics and Space Administration, Washington, D.C., 309–317.
- Seguin, B., and Itier, B. (1983). "Using midday surface temperature to estimate daily evaporation from satellite thermal IR data." *Int. J. Remote Sens.*, 4, 371–383.
- Soer, G. (1980). "Estimation of regional evapotranspiration and soil moisture conditions using remotely sensed crop surface temperatures." *Remote Sens. Environ.*, 9, 27–45.
- Su, Z. (2002). "The surface energy balance system (SEBS) for estimation of the turbulent heat fluxes." *Hydrology Earth Syst. Sci.*, 6(1), 85–99.